EFFECT OF INLET AND OUTLET LOCATIONS ON TRANSVERSE MIXED CONVECTION INSIDE A VENTED ENCLOSURE

Sumon Saha[*], Md. Tofiqul Islam, Mohammad Ali, Md. Arif Hasan Mamun and M. Quamrul Islam
Department of Mechanical Engineering,
Bangladesh University of Engineering and Technology,
Dhaka-1000, Bangladesh.
*Corresponding address: sumonsaha@me.buet.ac.bd

Abstract: *Transverse mixed convection is studied numerically in a vented enclosure with constant heat flux from uniformly heated bottom wall. An external airflow enters the enclosure through an opening in one vertical wall and exits from another opening in the opposite wall. The two-dimensional mathematical model includes the system of four partial differential equations of continuity, linear momentum and energy, solved by the finite element method. Flow fields are investigated by numerical simulations for air flowing with a Reynolds number in the range $50 \le Re \le 1000$, for Richardson numbers: $0 \le Ri \le 10$. Four different locations of inlet and outlets are introduced to analyze the effect of heat transfer in terms of velocity and temperature fields within the enclosure. The computational results show that the location of inlet and outlets alters significantly the temperature distribution in the flow fields and the heat transfer across the heated wall of the cavities. Empirical correlation is developed for relations using Nusselt number, Reynolds number and Richardson number, based on the enclosure height.*

Keywords: *Mixed convection, finite element method, vented enclosure, Richardson number.*

INTRODUCTION

Mixed convection flows and heat transfer in ventilated cavities are present in many transport processes in nature and in engineering devices. Examples of combined forced and free convection flows can be found in atmospheric flows, heat exchangers, nuclear reactors, solar energy storage and heat rejection systems, heaters, refrigeration devices, crystal growth, geothermal energy systems and cooling of electronic systems. In thermal control of electronic systems, air cooling are usually chosen for its simple design and low maintenance cost. Hence careful attention is necessary to ensure efficient design and minimizing power requirement for such cooing systems.

The effect of buoyancy on heat transfer in a forced flow is strongly influenced by the direction of the buoyancy force relative to that of the flow. Three special cases that have been studied extensively correspond to buoyancy-induced and forced motions having the same direction (assisting flow), opposite directions (opposing flow), and perpendicular directions (transverse flow). Heat transfer from vented enclosure with bottom heating has received increased attention for its importance in many engineering applications. For example, these include cooling of electronic components, finned heat exchangers, cavity of solar central receivers, as well as ventilation, evaporative cooling and fire control in buildings. However, most previous studies consider only natural convection or forced convection. Combined free and forced convection (or mixed convection) from vented cavities, although frequently encountered in engineering applications, has received rather little attention. In addition, most available results are limited to a simplified problem in which convective flow is induced in case of side heating of an open enclosure.

Nomenclature

C_p	specific heat of the fluid at constant pressure	x, y	Cartesian coordinates
D	height of the vertical sidewall	X, Y	non-dimensional Cartesian coordinates
g	gravitational acceleration	W	Height of the inlet and outlet openings
Gr	Grashof number		
h	convective heat transfer coefficient	**Greek symbols**	
k	thermal conductivity	α	thermal diffusivity
Nu	average Nusselt number	β	thermal expansion coefficient
p	pressure	υ	kinematic viscosity of the fluid
P	non-dimensional pressure	ρ	density of the fluid
Pr	Prandtl number		
q	heat flux	**Subscripts**	
Ra	Rayleigh number	i	inlet state
Re	Reynolds number	max	maximum
Ri	Richardson number	l	local
t	temperature	av	average
T	non-dimensional temperature	s	heated surface
u, v	velocity components		
U, V	non-dimensional velocity components		
$\overline{V}$	cavity volume		

A literature review concerning ventilated enclosures shows that some available works have considered the problem of mixed convection in rectangular cavities. The fluid dynamic and temperature fields in a reservoir were numerically simulated by Oberkampf and Crow[1]. The flow in the rectangular reservoir was assumed to be two-dimensional in a vertical plane. Inflow was allowed at the surface on one end and outflow occurred at any depth on the opposite end. The reservoir inflow was set at a given temperature and velocity. At the surface of the reservoir wind shear, short- and long-wave radiation, evaporation, and convective heat transfer were taken into account. The effects of inflow and outflow wind shear, and heat transfer on the reservoir were discussed.

Papanicolaou and Jaluria[2-6] carried out a series of numerical studies in order to investigate the combined forced and natural convective cooling of heat-dissipating electronic components located in a rectangular enclosure, and cooled by an external through-flow of air. Later, Lee et al[7] applied a finite element methods (FEMs) and a k-ε model to study the case of a rectangular open cavity. Their results, obtained only for one inlet-outlet location, showed that air cooling is not effective in laminar mixed convection. A related study of mixed convection in a partially divided rectangular enclosure was numerically studied also by Hsu et al[8]. It was observed that the heat transfer coefficient decreased rather rapidly as the height of the partition is more than about half of the total height of the enclosure. Calmidi and Mahajan[9] reported a numerical study of mixed convection on a heated horizontal surface within a partially open vertical enclosure using air as the working fluid. Two values of the Grashof number, 10^4 and 10^5, were considered for different Reynolds numbers, thus different ratios of Gr/Re^2 were calculated. They found that choosing the correct location for the exit boundary was crucial to the accuracy of the quantitative results.

A numerical study of an enclosure with a heated vertical plate located in the cavity was carried out by Hsu and Wang[10]. Discrete heat sources were embedded on the plate and different orientations were considered. When the heat source was embedded on the surface of the board opposite to forced flow inlet, the value of the convective Nusselt number was found to be independent of the location of the heat source. Omri and Nasrallah[11] studied mixed convection in a rectangular enclosure with differentially heated vertical side walls having openings for inlet and outlet. Two different placement configurations of the inlet and outlet openings on the side walls were investigated. In the first case the cold air was injected at the top of the hot wall and exited at the bottom of the cold wall, whereas in the second configuration the injection was at the lower edge of the hot wall and the exit was at the top of the cold wall. Improvement in cooling efficiency was found with the inlet placed at the bottom of the hot wall. Similar investigations were also carried out by Singh and Sharif[12] considering six placement configurations of the inlet and outlet openings. They observed that maximum cooling effectiveness is achieved if the inlet is kept near the bottom of the cold wall while the outlet is placed near the top of the hot wall.

Laminar mixed convection in a two-dimensional enclosure heated from one sidewall and submitted to an either aiding or opposing jet was numerically studied in the work of Angirasa[13] and Raji and Hasnaoui[14, 15]. Later, Raji and Hasnaoui[16] investigated the mixed convection in ventilated cavities where the horizontal top wall and the vertical left wall were prescribed with equal heat fluxes. Similar investigations are also carried out by the same authors[17] taking into consideration the effect of the thermal radiation on mixed convection.

A numerical study of mixed convection in open-ended enclosure has been investigated by Khanafer et al[18] for three different forced flow angle of attack. Results were obtained for Reynolds numbers in the range from 10^2 to 10^4, Grashof numbers between 10^2 and 10^5, and aspect ratio in the range from 0.25 to 1.0. It was shown that the average Nusselt numbers on the lower and upper surface increased almost linearly with Reynolds numbers for the three configurations at low Grashof numbers. A very interesting result was that the horizontal flow could be used to insulate the cavity from the surrounding medium thus minimizing the heat transfer between the cavity and the surroundings. Three-dimensional model of mixed convection in an air-cooled cavity has been studied by Moraga and Lopez[19] recently to examine the variations present in the results of two-dimensional models.

(a) BB Configuration

(b) BT Configuration

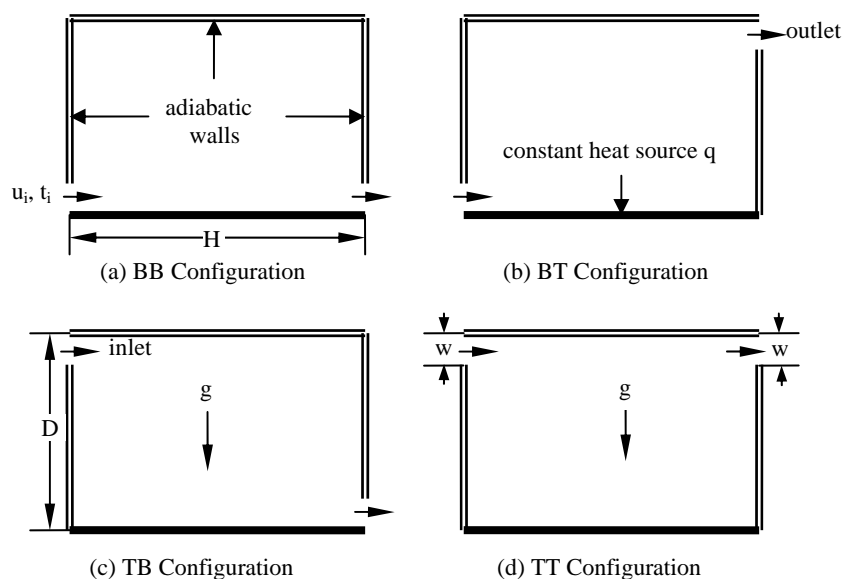(c) TB Configuration

(d) TT Configuration

Figure 1. Schematic flow configuration of the studied enclosures

Sahoo and Sharif[20] have been carried out a numerical simulation of laminar mixed-convective cooling of an isothermal hot surface by confined slot jet impingement. They observed that the average Nusselt number at the hot surface increases with increasing jet exit Reynolds number but has no significant change with Richardson number. Leong et al[21] carried out numerical simulation for mixed convection from an open cavity in a horizontal channel with various aspect ratios. They found that the Reynolds number and Grashof number control the flow pattern and the occurrence of recirculating cells while the aspect ratio has a significant influence on the orientation of these cells. Both numerical and experimental investigations were performed for mixed convection in a channel with an open cavity by Manca et al[22, 23]. The effect of heated wall position on convective heat transfer for different heating modes were analyzed numerically whereas experimental results reported the variation of aspect ratio of both the cavity and the channel gap. Most recently, Mahmud and Pop[24] have been investigated steady mixed convection in a square vented enclosure filled with a fluid-saturated porous medium for a wide range of Rayleigh number, Peclet number and the width of the inlet as a fraction of the height of the enclosure.

The literature review on the present subject found a limited number of works related to transverse flows in ventilated cavities. Hence the purpose of this research is to contribute to fill the void on studies done on this subject and to enhance the knowledge already acquired in this field, since the determination of heat exchange between the fluid and active walls is of importance in many engineering applications. In the present work, a mixed convection heat transfer problem is solved numerically by considering a cavity with two openings, and with a heat source at the bottom of the cavity. Problems in cavities with different placement of inlet and exit ports have been studied extensively here. The present investigation has been carried out to study the recirculations in the flow field, temperature distributions within the enclosure and heat transfer rate at the heated wall in terms of average Nusselt number when the bottom wall is uniformly heated and the top and other side walls are insulated. Finally an empirical correlation equation is developed to suit for the best configuration of the mixed convection modes.

PHYSICAL MODEL

A schematic representation of the studied configurations is depicted in Figures 1(a-d). Each of them is a rectangular enclosure ($D \times H$) with its bottom wall submitted to a uniform heat flux, q. The remaining walls are considered adiabatic. The cavity presented in Figure 1(a) is subjected to an external flow entering into the cavity from the bottom of the left insulated wall and leaving it from the bottom of the opposite vertical one. For brevity's sake, this configuration will be referred to as BB from now on. When the horizontal cold jet enters into the enclosure form the top of the insulated side wall and leaves from the top of the opposite vertical one (Figure 1(d)), this configuration will be referred to as TT. Similarly, other two configurations will be referred to as BT (Figure 1(b)) and TB (Figure 1(c)) respectively. The gravitational acceleration acts parallel to the side walls.

The values that were chosen originally for the geometric parameters of the problem to represent a typical

system of interest in the cooling of electronic equipment (see Fig. 1), are as follows: aspect ratio of the cavity, H/D = 1.5 and ratio of the size of inlet / outlet opening to the enclosure height, $w/D = 0.1$. Air injection through the inlet opening is in the horizontal direction with velocities $u = u_i$, $v = 0$ and a uniform temperature t_i. The outflow is assumed to have zero diffusion flux for all variables (outflow boundary condition).

MATHEMATICAL MODEL
Governing Equations:

The flow is considered to be two dimensional, steady and laminar, and the physical properties are assumed to be constant except for the density in the buoyancy term of the momentum equation in the vertical direction, which is treated by using the Boussinesq approximation. The viscous dissipation and joule heating in the energy equation is neglected. The working fluid is assumed to be air ($Pr = 0.71$). Taking into account the above mentioned assumptions, the governing equations can be written in non-dimensional form as follows:

Continuity equation:
$$\frac{\partial U}{\partial X} + \frac{\partial V}{\partial Y} = 0 \tag{1}$$

X-momentum equation:
$$U\frac{\partial U}{\partial X} + V\frac{\partial U}{\partial Y} = -\frac{\partial P}{\partial X} + \frac{1}{Re}\left(\frac{\partial^2 U}{\partial X^2} + \frac{\partial^2 U}{\partial Y^2}\right) \tag{2}$$

Y-momentum equation:
$$U\frac{\partial V}{\partial X} + V\frac{\partial V}{\partial Y} = -\frac{\partial P}{\partial Y} + \frac{1}{Re}\left(\frac{\partial^2 V}{\partial X^2} + \frac{\partial^2 V}{\partial Y^2}\right) + \frac{Gr}{Re^2}T \tag{3}$$

Energy equation:
$$U\frac{\partial T}{\partial X} + V\frac{\partial T}{\partial Y} = \frac{1}{RePr}\left(\frac{\partial^2 T}{\partial X^2} + \frac{\partial^2 T}{\partial Y^2}\right) \tag{4}$$

The mixed convection parameter seen in the above equation, Gr/Re^2, is also called as Richardson number, Ri. Note that the Grashof number is base on heat flux rather than on temperature difference because the constant heat flux type of boundary condition is considered for the heating element at the bottom wall. The non-dimensional numbers seen in the equations above, Re, Gr, and Pr, are Reynolds number, Grashof number, and Prandtl number, respectively, and they are defined as

$$Re = \frac{U_i H}{\upsilon} \qquad Gr = \frac{g\beta q H^3}{k\upsilon^2} \qquad Pr = \frac{\upsilon}{\alpha} \tag{5}$$

The dimensionless parameters in the equations above are defined as follows:

$$X = \frac{x}{H} \quad Y = \frac{y}{H} \quad U = \frac{u}{u_i} \quad V = \frac{v}{u_i} \quad P = \frac{p}{\rho u_i^2} \quad T = \frac{t - t_i}{(qH/k)} \tag{6}$$

where β, υ, and α are the coefficient of volumetric expansion, kinematic viscosity, and thermal diffusivity, respectively.

Boundary Conditions:

The boundary conditions used in this study are given in dimensionless form in Table 1. For velocities, no slip boundary conditions are adopted, i.e., horizontal and vertical velocity components, u and v, are set to zero at the

stationary walls. For temperatures, either adiabatic or constant heat flux boundary conditions are implemented at the wall surface. Both velocity and temperature are specified at the inlet of the enclosure but for the outlet, the outflow boundary conditions are implemented as described by Papanicolaou and Jaluria[3] and later by Moraga and López[19].

Table 1: The Boundary Conditions Implemented

	Temperature, T	Horizontal velocity, U	Vertical velocity, V
Inlet	0	1	0
Outlet	$\partial T/\partial X = 0$	$\partial U/\partial X = 0$	0
Bottom wall	$\partial T/\partial Y = 0$	0	0
Top wall	$\partial T/\partial Y = -1$	0	0
Side walls	$\partial T/\partial X = 0$	0	0

Heat Transfer:

The local heat transfer coefficient on the heat source surface is defined in terms of the inlet air temperature t_i as

$$h_l = \frac{q}{t_s(x) - t_i} \qquad (7)$$

where $t_s(x)$ is the local temperature of the heat source. The average heat transfer coefficient h_{av} is given as

$$h_{av} = \frac{1}{H} \int_0^H h_l \, dx \qquad (8)$$

The Nusselt number, Nu at the hot surface is a measure of convective heat transfer coefficient at the surface. The average Nusselt number is obtained using the expression

$$Nu = \frac{h_{av} H}{k} = \frac{D}{H} \int_0^{H/D} \frac{1}{T_S(X)} \, dX \qquad (9)$$

An index of cooling effectiveness is the bulk average temperature, which is defined as

$$T_{av} = \frac{1}{\overline{V}} \int T \, d\overline{V} \qquad (10)$$

where $\overline{V}$ is the cavity volume. For effective cooling, the average Nusselt number at the hot wall should be higher and bulk average fluid temperature should be lower.

NUMERICAL PROCEDURE

The numerical solutions of the governing model equations have been obtained using the software package FEMLAB. It is a MATLAB-based platform and relies on the finite element method (FEM) to discretise and solve the partial differential equations. The software can run the finite element analysis together with adaptive meshing and error control according to a variety of iterative numerical solvers. The applicability, validity and robustness of the code have been addressed by a number of previous works[25,26]. The use of FEM allows mass conservation in the domain; therefore, 'numerical loss' of mass in the computational domain is not a major concern. This section details both the model formulation and also the FEM solution of the problem. The problem was formulated using two different geometries in a coupled FEMLAB model incorporating "Convection & Conduction heat transfer" mode and a steady state "Incompressible Navier Stokes" mode. In FEMLAB, the nonlinear equations were solved iteratively using Broyden's method with an LU-decomposition pre-conditioner, always starting from a solution for a nearby Richardson number. A stationary non-linear solver was used together with Direct (UMFPACK) linear system solver. The relative tolerance for the error criteria was 1×10^{-4} and because the dependent variables vary greatly in magnitude, manual scaling of the dependent variables was used to improve numerical convergence. The manual scaling values are kept constant and were selected such that the magnitude of the scaled degrees of freedom was equal to one.

Grid refinement check:

A grid independence test is carried out to determine the appropriate grid size. Test for accuracy of grid fineness is obtained for non-uniform elements of nodes 25648, 39103, 48762, 58380 and 75191 nodes as is shown in Table 2. In these calculations, the percentage differences in the numerical results give a maximum of 0.0002% between 48762 and 75191 nodes. The coarse element (25648 nodes) yields a lower *Nu* (0.0014% lower) and higher dimensionless average bulk temperature (0.007% higher).
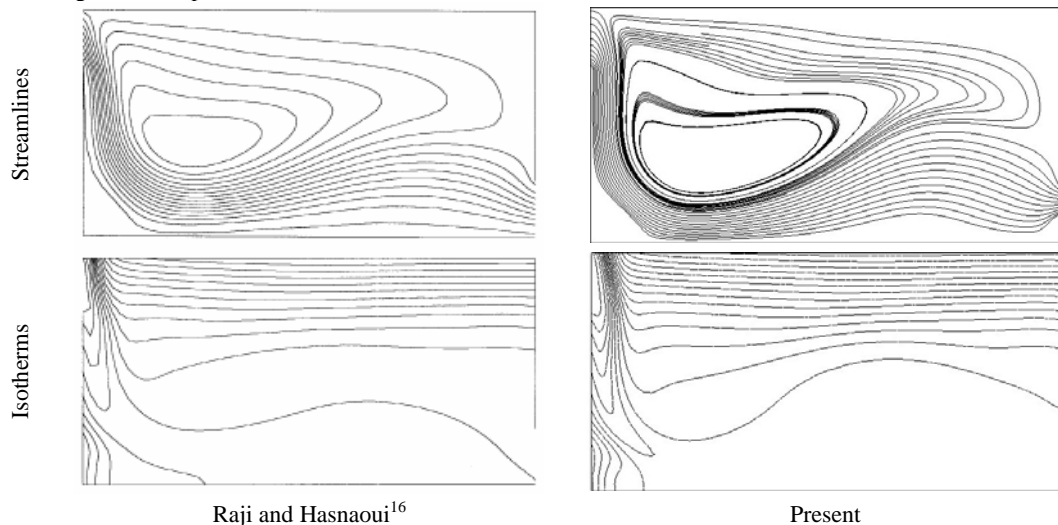

Figure 2. Comparison of streamlines and isotherms for validation at Pr = 0.72, Re = 100, Ra = 10^6 with the results of Raji and Hasnaoui[16]

However, a 48762 node grid required approximately six times less computational effort than the 75191 nodes of elements. Therefore, the 48762 nodes of element were chosen as a result of accuracy and efficiency.

Table 2. Comparison of the Results for Various Grid Dimensions (*Re* = 100, *Ri* = 1, *H/D* =1)

Nodes	Nu	T_{max}
25648	2.780109	0.449152
39103	2.780190	0.44910
48762	2.780160	0.449124
58380	2.780153	0.449123
75191	2.780149	0.449121

Code validation:

The computations of Raji and Hasnaoui[16] for mixed convection in a uniformly heated rectangular enclosure were validated and found to agree quite well. Figure 2 shows the comparison of streamline and isotherms of present model with that obtained by Raji and Hasnaoui[16]. Moreover, another numerical solution of Manca et al[23] were reproduced, and excellent agreement was found as mentioned in Table 3.

Table 3. Comparison of the Results for Validations at *Re* = 100, *H/D* = 1and *Pr* = 0.7

Parameters	Present		Manca et al.[23]	
	$Ri = 0.1$	$Ri = 10$	$Ri = 0.1$	$Ri = 10$
Nu	1.633	2.693	1.648	-
T_{max}	1.066	0.618	1.060	0.613

RESULTS AND DISCUSSION

In the present work, results were obtained for mixed convective flow for *Pr* = 0.71 and *Re* = 50, 100, 500 and 1000, respectively, using a non-uniform triangular mesh. The Richardson number, in the range $0 \leq Ri \leq 10$ at different inlet and outlet configurations, serves as a measure of the relative importance and natural convection modes on the heat transfer. The objective of this study is to examine the heat transfer and fluid flow characteristics due to mixed convection inside a rectangular vented enclosure with a constant heat flux heat source, mounted flush with the bottom wall. The resulting flow structure is analyzed to provide a fundamental understanding of the effect of Richardson number and Reynolds number on the flow and thermal fields. Important dimensionless parameter for the present study is the overall Nusselt number (*Nu*), on which the effect of Richardson number and Reynolds number is studied.

Characteristics of Flow and Thermal Fields:

(a) BT Configuration (Ventilation by the Bottom and Exit by the Top):

The effect of *Ri* and *Re* on isotherms and streamlines are shown in Figure 3. The basic flow structure in the absence of the free convection effect for *Ri* = 0 is presented in the top of the first column of Figure 3. The corresponding isotherms result from combined effects of
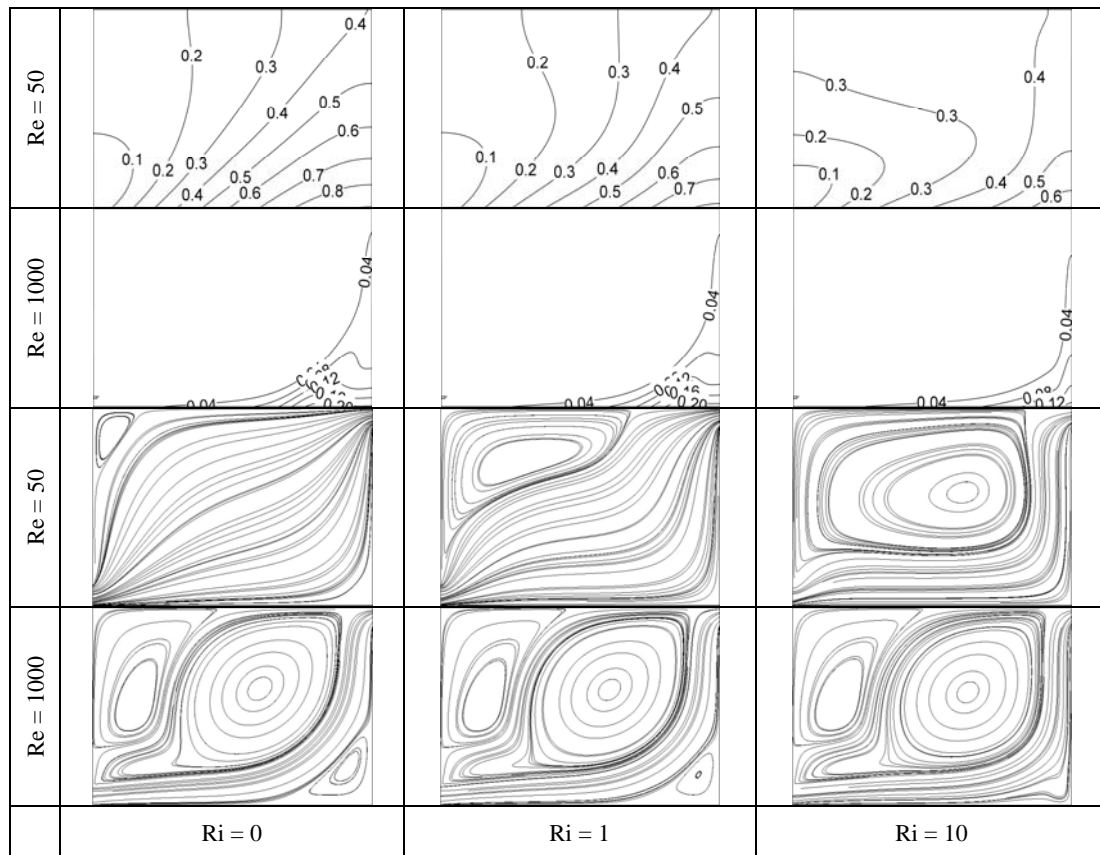

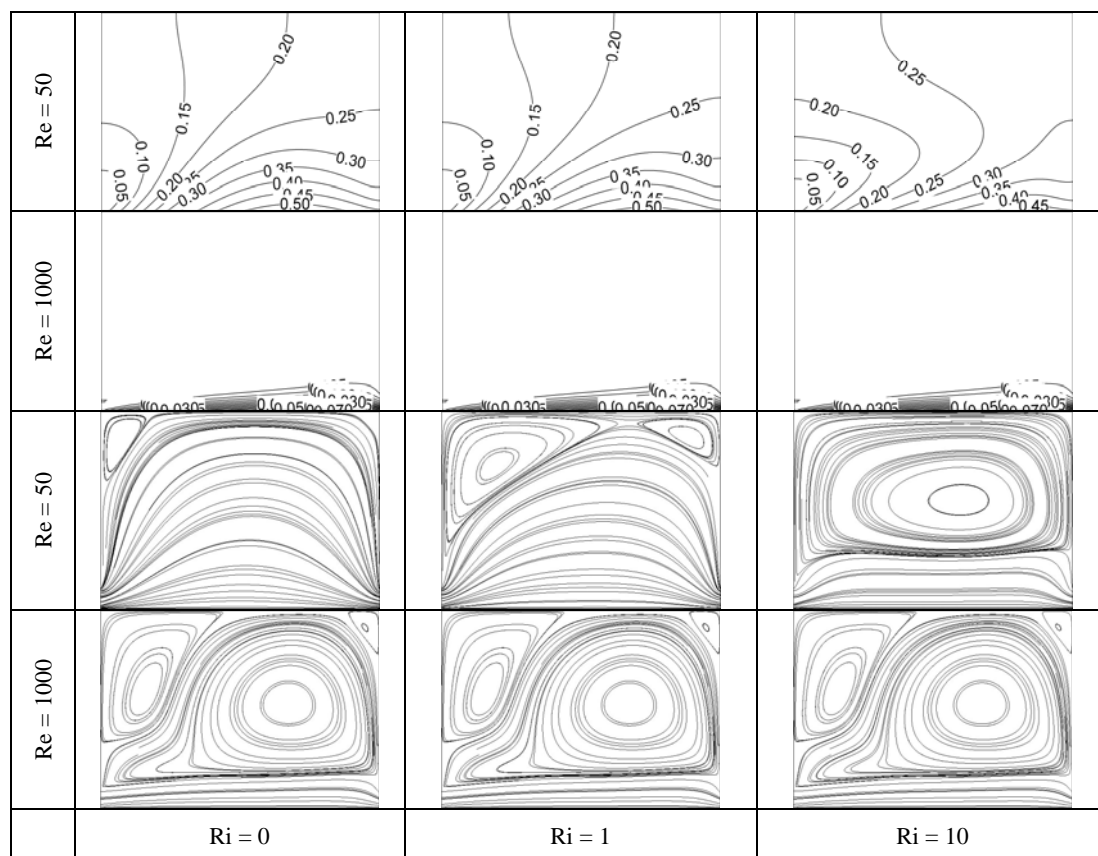Figure 3. Isotherms and Streamlines for configuration BT

Figure 4. Isotherms and Streamlines for configuration BB

conduction and forced convection. At $Ri = 0$ and $Re = 50$ while the induced flow enters into cavity through small inlet area, sudden expansion of the bulk fluid is occurred due to pressure rise into the cavity. Thus the bulk fluid occupies most of the part of the cavity. A very small vortex of very low speed appears at the left top corner of the cavity. Here heat is carried out by conduction due to kinetic energy drop in the bulk fluid, less mass in contact with the bottom heat source and thermally saturated fluid in the cavity for lower Re. For $Ri = 1$, it can be seen from Figure 3 that the natural convection effect is present but remains relatively weak at high Re, since the open lines characterizing the imposed flow are still dominant. Further increase of Ri gradually develops the recirculating cell, located at the left top corner of the cavity and leads to a large change in the streamline structure. This expansion of recirculating cell squeezes the induced forced flow path resulting almost same kinetic energy in the bulk induced flow as that of the inlet section. Convection heat transfer introduces with the growth of the recirculating cell resulting the faster removal of heat from the heat source. It must be noticed that when the buoyancy force increases with the increase of heat flux, the recirculation zone begins to develop by absorbing the thermal energy through the induced forced flow. Thereby the squeezed induced flow covers the whole part of the heat source at higher Ri. Hence for $Re \leq 500$ and $Ri = 10$, Figure 3 shows the existence of a large closed cells filling the entire cavity attributed to natural convection, which competes with the other modes of heat transfer (conduction and forced convection). Similarly, the effect of natural convection on the temperature distribution is characterized by the displacement of the isotherms front throughout the cavity. For $Re \geq 500$, two major recirculating cells of opposite

directions of angular motion are visualized. This is due to the higher inertia of the induced forced flow in the cavity resulting negative pressure in the upper part of the cavity and the shear effect. The isotherms in Figure 3 show that at low Re, the temperature at the right side near the heat source is higher because very small part of the bulk fluid, having relatively no motion, is trapped there. At higher Re, the induced flow passes through the heat source completely and thus the temperature at the right lower corner of the cavity decreases indicating better heat transfer. At low Ri and Re, the isotherms are almost uniformly distributed all over the cavity, indicating both conduction and convection heat transfer. As Ri increases, nonlinearity of the isotherms becomes higher and plume formation is profound, indicating the well established natural convection heat transfer. With the increase of Re, forced convection is predominating over the natural convection even at higher Ri. The isotherms are clustered near the heat source which points to the conduction heat transfer at the vicinity of the heat source and right insulated wall of the cavity and the remaining part of the cavity remains unchanged.

(b) BB Configuration (Ventilation by the Bottom and Exit by the Bottom):

Figure 4 present the thermal and flow fields as a function of the Richardson number and Reynolds number. At $Ri = 0$ and low Re, the bulk induced flow expands in the cavity resulting increase in potential energy. Heat is carried out merely by forced convection. Here very small recirculation cell of low velocity is formed at the top left corner of the cavity. An increase in the value of Ri, through an increase in Gr, leads to denser isothermal lines because of the increasing recirculation. Thus the isothermal lines
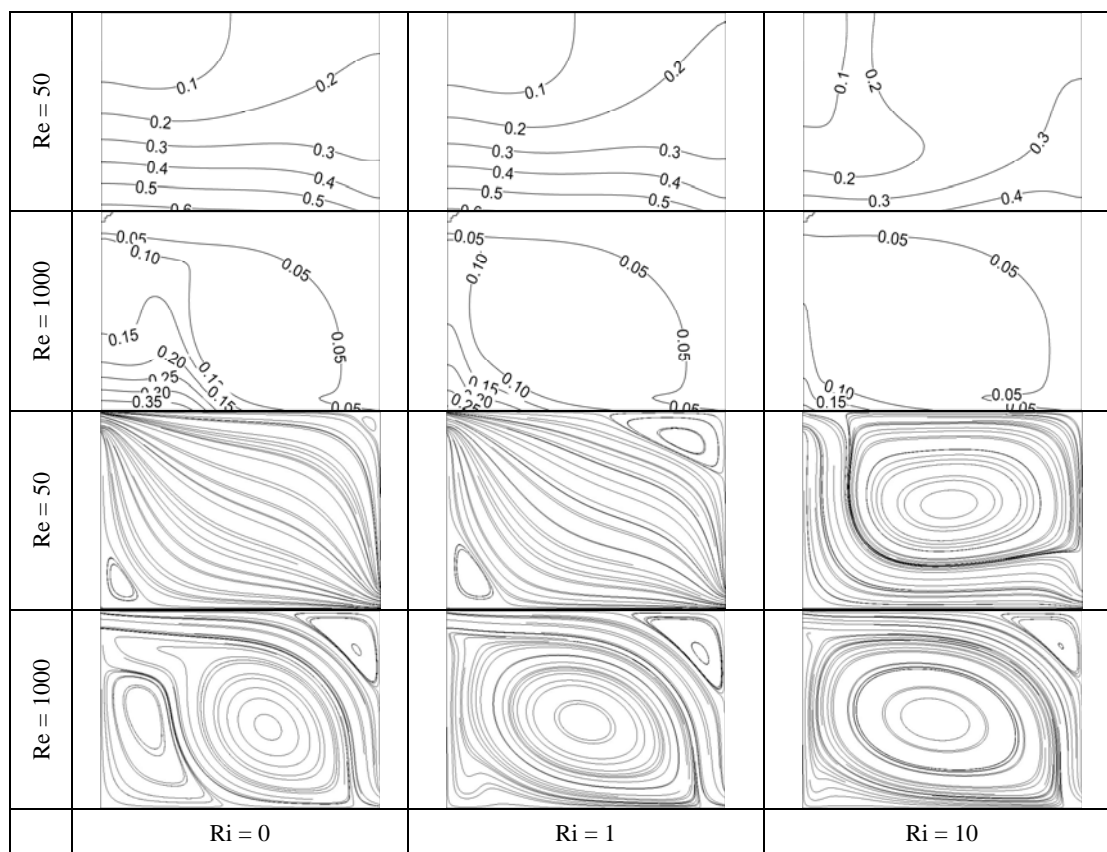
Figure 5. Isotherms and Streamlines for configuration TB

concentrate at the heat source for $Re \geq 500$ and $Ri = 10$ as shown in Figure 4. Making a comparison of isothermal lines at $Re = 1000$ for various Ri, no significant difference is found except that the dense isotherms at low Ri are shifted leftward. As Re increases, two recirculation cells are formed. Due to higher inertia, the fluid flows over the heated zone so faster that conducted heat in the induced flow cannot propagate to the recirculation. This phenomenon gives rise to negative pressure at the upper part of the cavity resulting two recirculating cells. With the increase of Re, natural convection is overwhelmed by the forced convection. In the absence of buoyancy effect, the isotherms are stratified inside the cavity when Re is low. As the buoyancy effect increases, isotherms are nonlinear and plume is formed. At higher Ri, the plume formation is profound indicating the supremacy of natural convection heat transfer over forced convection and conduction in the upper part of the cavity. With the increase of Re, the isotherms are bunched near the heat source resulting conductive heat transfer at the vicinity of the cavity and the thermal boundary layer at higher Re is thinner than that of lower Re. Heat is transferred solely by forced convection and conduction.

(c) TB Configuration (Ventilation by the Top and Exit by the Bottom):

Isotherms and streamlines illustrating the effect of Reynolds number and Richardson numbers are presented in Figure 5. For very low Ri and Re, the bulk induced fluid flows throughout the cavity and a pocket of fluid is formed at the lower part of the left insulated wall. Thus conduction and forced convection effects are dominant. At $Ri = 1$, the existence of two recirculation cells of very small size

indicates that natural convection is sprouted. For $Ri > 1$, the upper recirculation zone spreads and thereby squeezes the induced flow path, indicating a sign of supremacy of natural convection in the upper part of the cavity. But since the induced flow sweeps over the heat source, the forced convection acts as a driving force for the major heat removal. For $Re \geq 100$, the flow pattern is changed drastically, even in the absence of buoyancy effect, due to the influence of the induced flow. The lower trapped pocket of fluid is turned into a vortex near the left insulated wall due to the negative pressure. As Ri increases, the recirculation spreads. As a consequence, the induced flow is squeezed and the vortex almost covers the heat source indicating the dominance of the natural convective heat transfer. For $Re \geq 500$, the presence of a big cell rotating in the counter-clockwise direction and located below the open lines of the forced flow. It is noteworthy that the cold forced flow descends the heated bottom wall and imposes the rotation sense of the hot fluid in contact with the vertical active surface. The velocity of the descending fresh air is reduced by the heating effect of the horizontal active wall. At $Re = 1000$ and no buoyancy effect, the main stream is demarcated into four streams. These are two small vortexes of low speed, induced flow from the opening to the exit and large vortex of higher speed. Here induced natural convective current is dominant even at zero Ri. As Ri increases, the lower vortex merges to the large one and it almost covers the heat source. This scenario indicates that the forced convection is overwhelmed by the natural convective current. For zero buoyancy effect and low Re, the isotherms are stratified throughout the cavity indicating the diffusion heat transfer. As Ri increases, the isotherms become nonlinear and plume is formed which are the cryptogram of strong natural
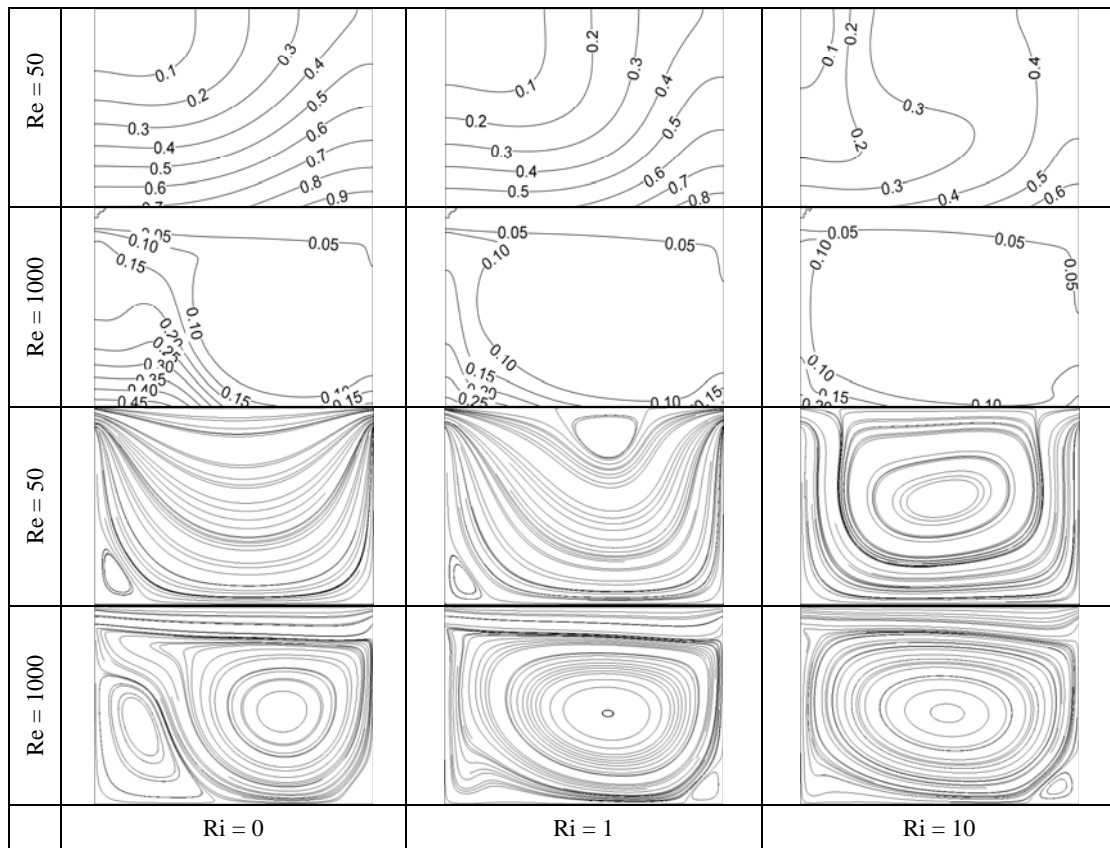
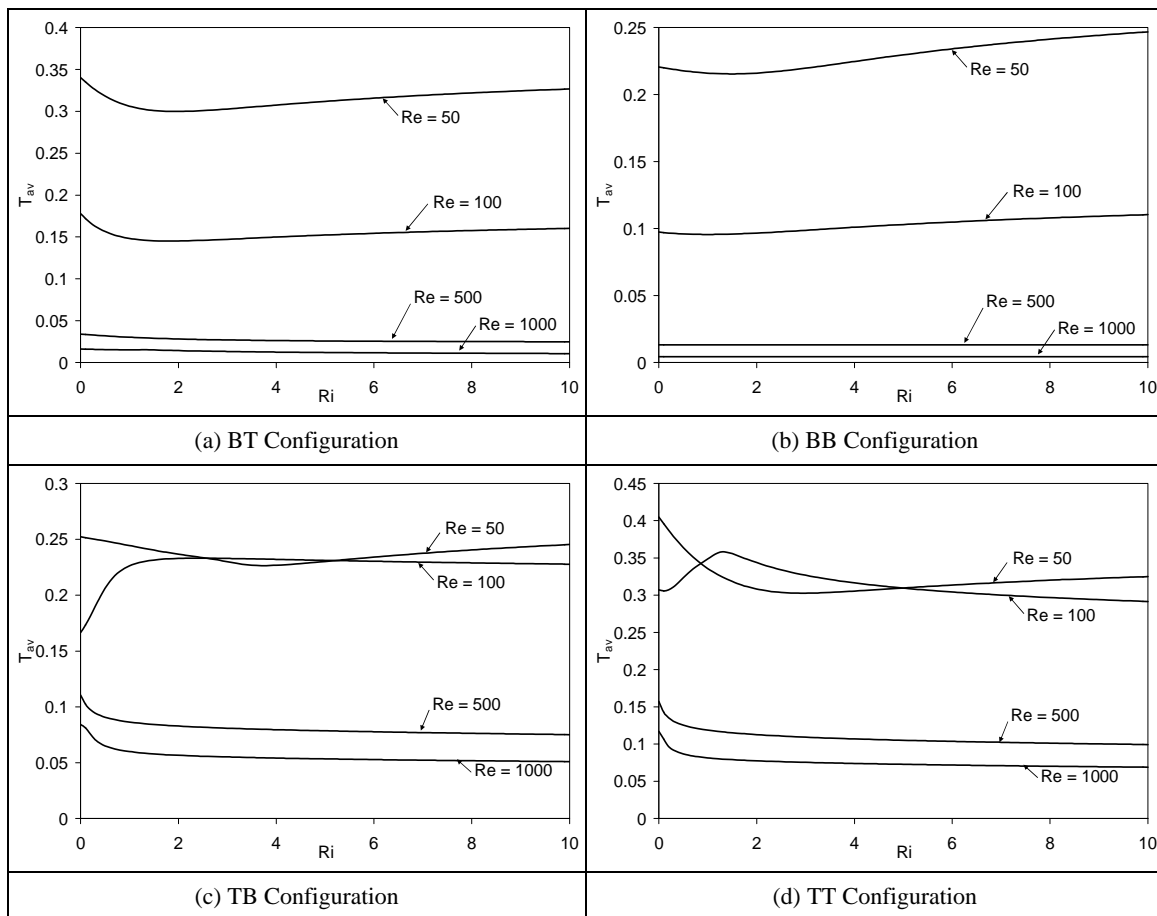Figure 6. Isotherms and Streamlines for configuration TT

Figure 7. Average bulk fluid temperature variation with different Reynolds numbers and Richardson numbers for four configurations.

convective effect. For $Re \geq 500$, the plume formation appears even at zero buoyancy effect and its intensity becomes higher with the increase of Ri. Little portion of heat is transferred by conduction near the left vicinity of the heated wall. Major portion of heat is carried out by natural convection rather than forced convection. In comparison with Figure 3 for case BT configuration, it is interesting to observe that the enclosure spreads with streamlines at $Re \geq 500$ in a similar manner except in the vicinity of the heat sources at the same value of Ri and $Re \leq 100$.

(d) TT Configuration (Ventilation by the Top and Exit by the Top):

The effect of the Reynolds number on fluid flow and temperature distribution is presented in Figures 6 for various Re and Ri. As shown in Figure 6, when Ri is increased for a given Re value, the lower isotherms go away from the exit when Ri is still low, but at larger Ri values the thermal field tends to go beyond buoyancy. The buoyancy forces, aiding the forced flow, improve mixing and enhance the thermal exchange. For $Re = 50$, Figure 6 shows the absence of thermal interaction between the forced flow and the heated wall. The effect of natural convection is characterized by the presence of two counter-rotating cells, leading to a good thermal stratification in the central part of the cavity. By increasing Re up to 500, a net variation of the flow structure is observed where the size and intensity of the lower closed cell are considerably affected. Further increase of the intensity of the jet leads to

the disappearance of the upper cell as shown in Figure 3 for $Re = 1000$. At $Ri = 0$ and $Re = 50$, the stream spreads out into the core more sharply in the lower region, giving rise to more or less a sudden expansion. For $Ri = 1$, two small vortexes are formed at the upper mid section of the cavity and the lower part of the insulated wall. As Ri increases, it evolves into a large one of high speed. Since induced flow covers the heat source, heat is carried out merely by forced convection. For $Re \geq 100$, a radical change is visualized in the flow field. The lower recirculating cell evolves into a large one of high speed with the increase of Ri. Thereby it squeezes the entrance stream to flow over it. Heat is carried out solely by natural convection due to the existence of the recirculating cell near the heated wall. The isotherms are almost linear and distributed inside the cavity at low Re and zero buoyancy effect. This points out to the conduction heat transfer. As Ri increases, nonlinearity of isotherms are seen. Plume formation are initiated which indicates the launch of natural convective current. For $Re \geq 500$, plume formation is found even at low Ri. As Ri increases, plume formation becomes profound. The isotherms are clustered near left side of the heat source which points to the conduction heat transfer at the vicinity of the heat source and the remaining part of the cavity remains cool.

Heat Transfer Characteristics:

The effect of Richardson number on the average bulk fluid temperature for different Reynolds number and configurations is shown in Figure 7. A similarity of
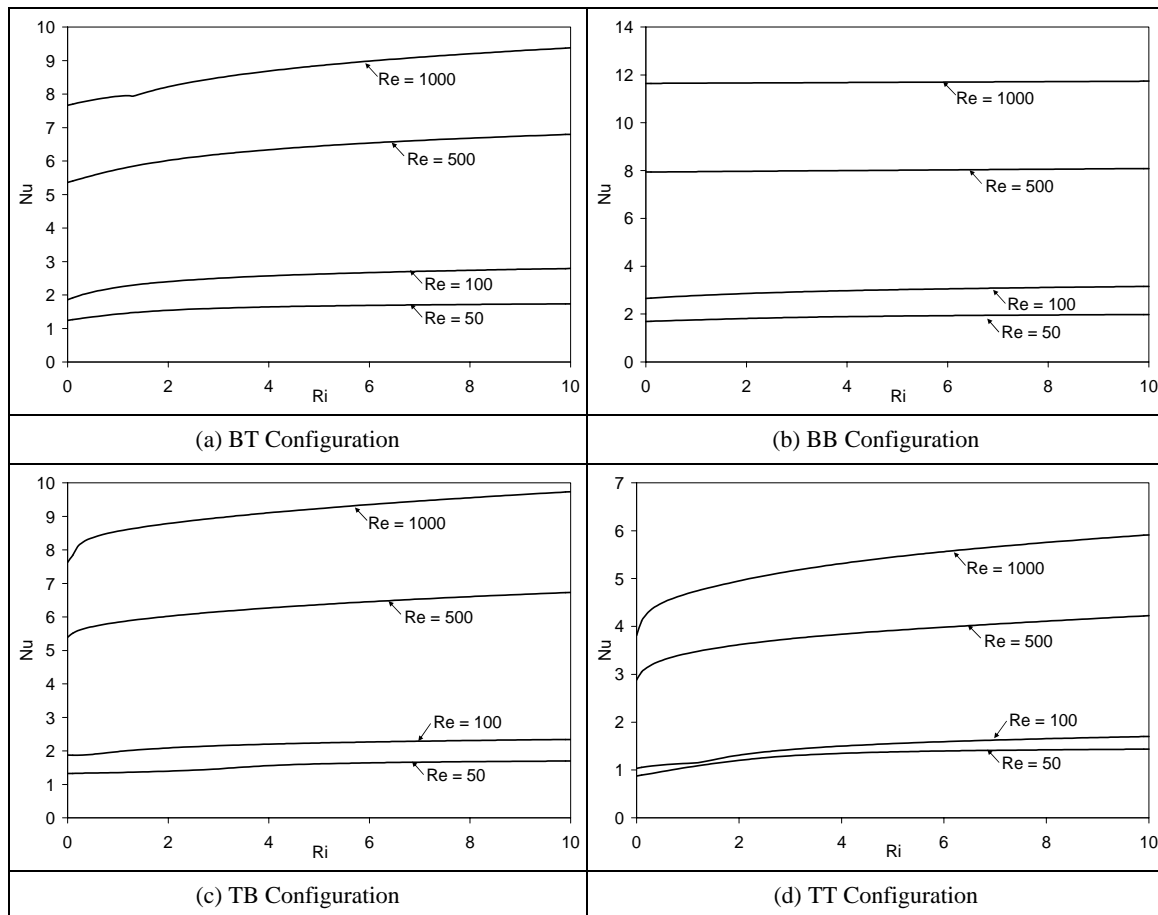

Figure 8. Average Nusselt number variation with different Reynolds numbers and Richardson numbers for four configurations.

average bulk fluid temperature is found between BT configuration and BB configuration. For both configurations, average bulk fluid temperature is independent of *Ri*. But for *Re* = 50 and 100, average bulk fluid temperature initially decreases for *Ri* ≤ 1 and then increases for 1 ≤ *Ri* ≤ 10. Higher average bulk fluid temperature is obtained for *Re* = 50 indicating poor heat transfer. But for *Re* = 500 and 1000, it is near to zero, which indicates better thermal performance due to higher Nusselt number. Since BB configuration has minimum average bulk fluid temperature among the others, it shows optimum heat transfer performance.

The effect of Richardson number on the average Nusselt number for different Reynolds number and configurations is shown in Figure 8. As *Ri* increases, average Nusselt number increases gradually for all values of *Re* in all configurations except BB configuration. In BB configuration, the average Nusselt number is independent of the *Ri* for all values of *Re*. Average Nusselt number is higher for the higher value of *Re*. Maximum average Nusselt number is obtained, without the effect of *Ri*, in BB configuration. This scenario of heat transfer is occurred because the induced forced flow passes over the heat source all over time. Thus heat transfer is enhanced by forced convection rather than natural convection.

Heat Transfer Correlation:

The average Nusselt numbers shown in Figure 8 are correlated in terms of Richardson number and Reynolds number for BB configuration as one of the best configuration in terms of higher heat transfer rate. The relationship is expressed as follows:

$$Nu = 0.086 Ri^{0.528} + 0.399 Re^{0.5} - 1.159 \qquad (11)$$

where 50 ≤ *Re* ≤ 1000, 0 ≤ *Ri* ≤ 10 and the maximum correlation coefficient is 0.99.

CONCLUSION

The effects of mixed convective flow on the thermal phenomena in an enclosure have been investigated. This study presents important fundamental aspects of mixed convection in an enclosure. The numerical results explain the importance of the orientation of the inlet and exit ports in the enclosure considered. Both *Re* and buoyancy parameter *Ri* largely affect the thermal characteristics. At higher value of *Re*, the value of *Nu* is independent of the variation of *Ri* for the most preferable BB configuration compare to other three configurations. On the other hand, similar heat transfer performance exist both for BT and TB configurations. The heat transfer coefficient is influenced significantly by the Reynolds number for all four configurations.

REFERENCES:

1. Oberkampf W.L. and Crow L.L., Numerical Study of the Velocity and Temperature Fields an a Flow-Through Reservoir, ASME J. Heat Transfer, Vol 98 (1976) p. 353-359.
2. Papanicolaou E. and Jaluria Y., Mixed Convection from an Isolated Heat Source in a Rectangular Enclosure, Numerical Heat Transfer, Part A, Vol 18 (1990) p. 427-461.
3. Papanicolaou E. and Jaluria Y., Transition to a Periodic Regime in Mixed Convection in a Square Cavity, J. Fluid Mech. Vol 239 (1992) p. 489-509.
4. Papanicolaou E. and Jaluria Y., Mixed Convection from a Localized Heat Source in a Cavity with Conducting Walls: A Numerical Study, Numerical Heat Transfer, Part A, Vol 23 (1993) p. 463–484.
5. Papanicolaou E. and Jaluria Y., Mixed Convection from Simulated Electronic Components at Varying Relative Positions in a Cavity, ASME J. Heat Transfer, Vol 116 (1994) p. 960-970.
6. Papanicolaou E. and Jaluria Y., Computation of Turbulent Flow in Mixed Convection in a Cavity with a Localized Heat Source, ASME J. Heat Transfer, Vol 117 (1995) p. 649-658.
7. Lee S.-C., Cheng C.-Y. and Chen C.-K., Finite Element Solutions of Laminar and Turbulent Flows with Forced and Mixed Convection in an Air-Cooled Room, Numerical Heat Transfer, Part A, Vol 31 (1997) p. 529–550.
8. Hsu T.-H., Hsu P.-T. and How S.-P., Mixed convection in a partially divided rectangular enclosure, Numerical Heat Transfer, Part A, Vol 31 (1997) p. 655–683.
9. Calmidi V.V. and Mahajan R.L., Mixed Convection Over a Heated Horizontal Surface in a Partial Enclosure, Int. J. Heat and Fluid Flow, Vol 19 (1998) p. 358-367.
10. Hsu T.H. and Wang S.G., Mixed Convection in a Rectangular Enclosure with Discrete Heat Sources, Numerical Heat Transfer, Part A, Vol 38 (2000) p. 627-652.
11. Omri A. and Nasrallah S.B., Control Volume Finite Element Numerical Simulation of Mixed Convection in an Air-Cooled Cavity, Numerical Heat Transfer, Part A, Vol 36 (1999) p. 615-637.
12. Singh S. and Sharif M.A.R., Mixed Convective Cooling of a Rectangular Cavity with Inlet and Exit Openings on Differentially Heated Side Walls, Numerical Heat Transfer, Part A, Vol 44 (2003) p. 233-253.
13. Angirasa D., Mixed Convection in A Vented Enclosure with an Isothermal Vertical Surface, Fluid Dynamics Research, Vol 26 (2000) p. 219-233.
14. Raji A. and Hasnaoui M., Correlations on Mixed Convection in Ventilated Cavities, Rev. Gen. Therm., Vol 37 (1998) p. 874-884.
15. Raji A. and Hasnaoui M., Mixed Convection Heat Transfer in a Rectangular Cavity Ventilated and Heated from the Side, Numerical Heat Transfer, Part A, Vol 33 (1998) p. 533-548.
16. Raji A. and Hasnaoui M., Mixed Convection Heat Transfer in Ventilated Cavities with Opposing and Assisting Flows, Engineering Computations, Vol 17 No. 5 (2000) p. 556-572.
17. Raji A. and Hasnaoui M., Combined Mixed Convection and Radiation in Ventilated Cavities, Engineering Computations, Vol 18 No. 7 (2001) p. 922-949.
18. Khanafer K., Vafai K. and Lightstone M., Mixed Convection Heat Transfer in Two Dimensional Open Ended Enclosures, Int. J. Heat and Mass Transfer, Vol 45 (2002) p. 5171-5190.
19. Moraga N.O. and López S.E., Numerical Simulation of Three-Dimensional Mixed Convection in an Air-Cooled Cavity, Numerical Heat Transfer, Part A, Vol 45 (2004) p. 811-824.

20. Sahoo D. and Sharif M.A.R., Mixed-Convective Cooling Of An Isothermal Hot Surface By Confined Slot Jet Impingement, Numerical Heat Transfer, Part A, Vol 45 (2004) p. 887-909.

21. Leong J.C., Brown N.M. and Lai F.C., Mixed Convection From an Open Cavity in a Horizontal Channel, Int. Comm. Heat and Mass Transfer, Vol 32 (2005), p. 583-592.

22. Manca O., Nardini S., Khanafer K. and Vafai K., Effect of Heated Wall Position on Mixed Convection in a Channel with an Open Cavity, Numerical Heat Transfer, Part A, Vol 43 (2003) p. 259-282.

23. Manca O., Nardini S. and Vafai K., Experimental Investigation of Mixed Convection in a Channel with an Open Cavity, Experimental Heat Transfer, Vol 19 (2006) p. 53-68.

24. Mahmud S. and Pop I., Mixed Convection in a Square Vented Enclosure Filled with a Porous Medium, Int. J. Heat and Mass Transfer, Vol 49 (2006) p. 2190-2206.

25. van Schijndel A.W.M., Modeling and Solving Building Physics Problems with Femlab, Building and Environment, Vol 38 (2003), p. 319-327.

26. FEMLAB 3.0a, COMSOL Inc., Burlington, MA, 2006. http://www.comsol.com.